

Phase transition in perovskite manganites with orbital degree of freedom

S. Okamoto, S. Ishihara, and S. Maekawa

Institute for Materials Research, Tohoku University, Sendai 980-8577, Japan

(Received 22 September 1999)

Roles of orbital degree of freedom of Mn ions in phase transition as functions of temperature and hole concentration in perovskite manganites are studied. It is shown that the orbital order-disorder transition is of the first order in the wide region of hole concentration, and the Néel temperature for the anisotropic spin ordering, such as the layer-type antiferromagnetic one, is lower than the orbital ordering temperature due to the anisotropy in the orbital space. The calculated results of the temperature dependence of the spin and orbital order parameters explain a variety of the experiments observed in manganites.

I. INTRODUCTION

Perovskite manganites $A_{1-x}B_x\text{MnO}_3$ (A represents La, Nd, or Pr, B represents Sr or Ca) and their related compounds have been studied extensively from both experimental and theoretical sides since the discovery of colossal magnetoresistance (CMR).¹⁻⁴ In particular, the gigantic decrease of the electrical resistivity is brought about in the vicinity of the transition from a spin, charge, and orbital ordered phase to a ferromagnetic metallic one with slightly changing temperature and/or by applying external fields.^{5,6} Thus, mechanism of such dramatic phenomena associated with the phase transition is the central issue of current studies. It is now accepted that CMR and its related phenomena are not understood within the simple double exchange scenario.⁷

The orbital degree of freedom in Mn ions is one of the convincing candidates to bring about a rich variety of phenomena in perovskite manganites. Due to the strong Hund coupling and the crystalline field, two e_g orbitals of a Mn ion, i.e., the $d_{3z^2-r^2}$ and $d_{x^2-y^2}$ orbitals, are degenerate and one of them is occupied by an electron in a Mn^{3+} ion. It is well known that the $(d_{3x^2-r^2}/d_{3y^2-r^2})$ -type orbital ordered state, where the two orbitals are alternately aligned, is realized in the undoped manganites LaMnO_3 .⁸⁻¹² Recently, the uniform alignment of the $d_{x^2-y^2}$ orbital in the layer (A)-type antiferromagnetic (AF) metal is experimentally confirmed in $\text{Pr}_{0.5}\text{Sr}_{0.5}\text{MnO}_3$, $\text{Nd}_{0.45}\text{Sr}_{0.55}\text{MnO}_3$ (Refs. 13-15), and $\text{La}_{1-x}\text{Sr}_x\text{MnO}_3$ with $x \sim 0.55$ (Ref. 16). It is recognized that the orbital degree of freedom controls the transport and optical properties in the metallic phase as well as the magnetic one.

In this paper, we study the phase transition in perovskite manganites based on the model where the orbital degree of freedom and electron correlation are included. By adopting the mean-field theory, roles of the orbital in the phase transitions are investigated as functions of temperature (T) and carrier concentration (x). Since there is a strong anisotropy in the orbital space unlike the spin one, the orbital order-disorder transition is of the first order in the wide range of x , and the Néel temperature T_N for the anisotropic spin ordering, such as the A -type AF one, is lower than the orbital ordering temperature T_{OO} . The calculated temperature dependence of the spin and orbital order parameters explains a variety of experiments in manganites.

In Sec. II, the model Hamiltonian is derived and the mean-field theory at finite T is introduced. In Sec. III, the numerical results of the spin and orbital phase diagram are presented. We focus on the phase transitions in (i) a lightly doped region where the ferromagnetic Curie temperature, T_C , and T_{OO} are close with each other and (ii) a highly doped region where the A -type AF state accompanied with the $d_{x^2-y^2}$ orbital appears. In Sec. IV, the phase transitions are studied analytically by expanding the free energy with respect to the spin and orbital order parameters. Section V is devoted to the summary and discussion.

II. MODEL AND FORMULATION

Let us set up the model Hamiltonian describing the electronic structure in manganites. We consider the tight-binding Hamiltonian in the cubic lattice consisting of Mn ions. At each site, two e_g orbitals are introduced and t_{2g} electrons are treated as a localized spin ($\vec{S}_{t_{2g}}$) with $S=3/2$. We introduce three kinds of Coulomb interaction between e_g electrons at the same site, i.e., the intraorbital Coulomb interaction (U), the interorbital interaction (U'), and the exchange interaction (I). The hopping integral between site i with orbital γ and its nearest-neighbor site j with γ' is denoted by $t_{ij}^{\gamma\gamma'}$. The Hund coupling (J_H) between e_g and t_{2g} spins and the antiferromagnetic superexchange (SE) interaction (J_{AF}) between nearest-neighbor t_{2g} spins are also introduced. Among these parameters, the intrasite Coulomb interactions are the largest. Thus, by excluding the doubly occupied state in the e_g orbitals, we derive the effective Hamiltonian describing the low-energy electronic states,¹⁷

$$\mathcal{H} = \mathcal{H}_t + \mathcal{H}_J + \mathcal{H}_H + \mathcal{H}_{AF}. \quad (1)$$

The first and second terms correspond to the so-called t and J terms in the tJ model and are given by

$$\mathcal{H}_t = \sum_{\langle ij \rangle \gamma \gamma' \sigma} t_{ij}^{\gamma\gamma'} \tilde{d}_{i\gamma\sigma}^\dagger \tilde{d}_{j\gamma'\sigma} + \text{H.c.}, \quad (2)$$

and

$$\begin{aligned} \mathcal{H}_J = & -2J_1 \sum_{\langle ij \rangle} \left(\frac{3}{4} n_i n_j + \vec{S}_i \cdot \vec{S}_j \right) \left(\frac{1}{4} - \tau_i^l \tau_j^l \right) \\ & - 2J_2 \sum_{\langle ij \rangle} \left(\frac{1}{4} n_i n_j - \vec{S}_i \cdot \vec{S}_j \right) \left(\frac{3}{4} + \tau_i^l \tau_j^l + \tau_i^l + \tau_j^l \right), \end{aligned} \quad (3)$$

respectively. Here, $\tau_i^l = \cos[(2\pi/3)m_l]T_{iz} - \sin[(2\pi/3)m_l]T_{ix}$ and $(m_x, m_y, m_z) = (1, -1, 0)$. l denotes a direction of the bond connecting site i and site j . $\tilde{d}_{i\gamma\sigma}$ is the annihilation operator of the e_g electron at site i with spin σ and orbital γ with excluding double occupancy of electron and n_i is the number operator defined as $n_i = \sum_{\gamma\sigma} \tilde{d}_{i\gamma\sigma}^\dagger \tilde{d}_{i\gamma\sigma}$. The explicit form of $t_{ij}^{\gamma\gamma'}$ is determined by the Slater-Koster formulas.¹⁸ \vec{S}_i is the spin operator of the e_g electron with $S=1/2$ and \vec{T}_i is the pseudospin one for the orbital degree of freedom defined as $\vec{T}_i = (1/2) \sum_{\gamma\gamma'\sigma} \tilde{d}_{i\gamma\sigma}^\dagger (\vec{\sigma})_{\gamma\gamma'} \tilde{d}_{i\gamma'\sigma}$ where $T_{iz} = +(-)1/2$ corresponds to the state where the $d_{3z^2-r^2}$ ($d_{x^2-y^2}$) orbital is occupied by an electron. $J_1 = t_0^2/(U' - I)$ and $J_2 = t_0^2/(U' + I + 2J_H)$ where t_0 is the hopping integral between nearest-neighboring $d_{3z^2-r^2}$ orbitals in the z direction and $U = U' + I$ is assumed. The third and fourth terms in Eq. (1) represent the Hund coupling and the antiferromagnetic SE interaction, respectively, and are given by

$$\mathcal{H}_H + \mathcal{H}_{AF} = -J_H \sum_i \vec{S}_i \cdot \vec{S}_{t_{2g}i} + J_{AF} \sum_{\langle ij \rangle} \vec{S}_{t_{2g}i} \cdot \vec{S}_{t_{2g}j}. \quad (4)$$

The detailed derivation of the Hamiltonian is presented in Ref. 17. Characteristics of this Hamiltonian are summarized as follows: (1) the two kinds of magnetic interactions between spins of e_g electrons, i.e., the SE and double exchange interactions are described by \mathcal{H}_J and \mathcal{H}_I , respectively,¹⁹ (2) there is a strong anisotropy in the pseudospin space unlike the spin space, and (3) the first term in Eq. (3) is the dominant term in \mathcal{H}_J and stabilizes the ferromagnetic state associated with the antiferromagnetic-type orbital ordered one where different types of orbitals are alternately aligned.²⁰⁻²³ The interaction between the orbital degree of freedom and the Jahn-Teller (JT)-type lattice distortion is not included in this model by considering the following facts: (1) the cooperative JT distortion is rapidly diminished by doping holes in manganites with large bandwidth,²⁴ (2) in $\text{La}_{0.88}\text{Sr}_{0.12}\text{MnO}_3$, the orbital ordering is experimentally confirmed in the phase where the cooperative JT distortion is almost quenched,¹⁹ and (3) the linear coupling between the pseudospin and the JT-type distortion does not change the order of the phase transition at $x=0$. Effects of the higher-order coupling between the orbital and the lattice distortion are discussed in Sec. V.

Being based on the Hamiltonian, the spin and orbital states are studied at finite T and x . The mean-field theory proposed by de Gennes²⁵ is applied to the present system with orbital degeneracy and electron correlation.²⁶ In this theory, the spin and pseudospin operators are treated as classical vectors,

$$(S_{ix}, S_{iy}, S_{iz}) = \frac{1}{2} (\sin \theta_i^s \cos \phi_i^s, \sin \theta_i^s \sin \phi_i^s, \cos \theta_i^s), \quad (5)$$

and

$$(T_{ix}, T_{iy}, T_{iz}) = \frac{1}{2} (\sin \theta_i^t, 0, \cos \theta_i^t), \quad (6)$$

where $\theta_i^{s(t)}$ is the polar angle in the spin (orbital) space and ϕ_i^s is the azimuthal one in the spin space. A motion of the pseudospin is assumed to be confined in the xz plane and θ_i^t describes the orbital state at site i as follows:

$$|\theta_i^t\rangle = \cos \frac{\theta_i^t}{2} |3z^2 - r^2\rangle + \sin \frac{\theta_i^t}{2} |x^2 - y^2\rangle. \quad (7)$$

\vec{S}_i and \vec{T}_i are denoted by \vec{u}_i in the uniform fashion. A thermal distribution of \vec{u}_i is described by the distribution function,

$$w_i^u(\vec{u}_i) = \frac{1}{v_i^u} \exp \left(\vec{\lambda}_i^u \cdot \frac{\vec{u}_i}{|\vec{u}_i|} \right), \quad (8)$$

where $\vec{\lambda}_i^u$ is the mean field and v_i^u is the normalization factor given by

$$v_i^s = \int_0^\pi d\theta_i^s \int_0^{2\pi} d\phi_i^s \sin \theta_i^s \exp(|\vec{\lambda}_i^s| \cos \theta_i^s), \quad (9)$$

and

$$v_i^t = \int_0^{2\pi} d\theta_i^t \exp(|\vec{\lambda}_i^t| \cos \theta_i^t). \quad (10)$$

The free energy is given by a summation of the expectation value of the Hamiltonian and entropy,

$$\mathcal{F} = \langle \mathcal{H} \rangle_{st} - TN(\mathcal{S}^s + \mathcal{S}^t), \quad (11)$$

where N is the number of Mn ions and \mathcal{S}^u is the entropy for \vec{u} defined by

$$\mathcal{S}^u = -\langle \ln w^u(\vec{u}) \rangle_u. \quad (12)$$

$\langle A \rangle_u$ implies the expectation value of A with respect to the distribution function. $M_u = \langle \vec{u} \cdot \vec{\lambda}^u / (|\vec{u}| |\vec{\lambda}^u|) \rangle_u$ is adopted as an order parameter in $\langle \mathcal{H}_J \rangle_{st}$, $\langle \mathcal{H}_H \rangle_{st}$, and $\langle \mathcal{H}_{AF} \rangle_{st}$. The relation $3 \langle \vec{S}_i \rangle_s = \langle \vec{S}_{t_{2g}i} \rangle_s$ is assumed. As for $\langle \mathcal{H}_I \rangle_{st}$, the rotating frames in the spin and pseudospin spaces are introduced. The electron annihilation operator is decomposed as $\tilde{d}_{i\gamma\sigma} = z_{i\sigma}^s z_{i\gamma}^t h_i^\dagger$ where h_i^\dagger is the creation operator of a spin- and orbital-less fermion describing a hole motion and $z_{i\sigma}^{s(t)}$ is an element of the unitary matrix in the spin (pseudospin) frame.^{27,28} These are given by $z_{i\uparrow}^s = \cos(\theta_i^s/2) e^{-i\phi_i^s/2}$, $z_{i\downarrow}^s = \sin(\theta_i^s/2) e^{i\phi_i^s/2}$, $z_{ia}^t = \cos(\theta_i^t/2)$, and $z_{ib}^t = \sin(\theta_i^t/2)$. \mathcal{H}_I is rewritten as

$$\mathcal{H}_I = \sum_{\langle ij \rangle \sigma \gamma \gamma'} (z_{i\sigma}^{s*} z_{j\sigma}^s) (z_{i\gamma}^{t*} z_{j\gamma'}^t) h_i h_j^\dagger + \text{H.c.}, \quad (13)$$

and is diagonalized in the momentum space as follows:

$$\langle \mathcal{H}_I \rangle_{st} = \left\langle \sum_k \sum_{l=1}^{N_l} \varepsilon_k^l f_F(\varepsilon_k^l - \varepsilon_F) \right\rangle_{st}, \quad (14)$$

where ε_k^l is the energy in the l th band for the spinless and orbital-less fermion with momentum \vec{k} and N_l is the number

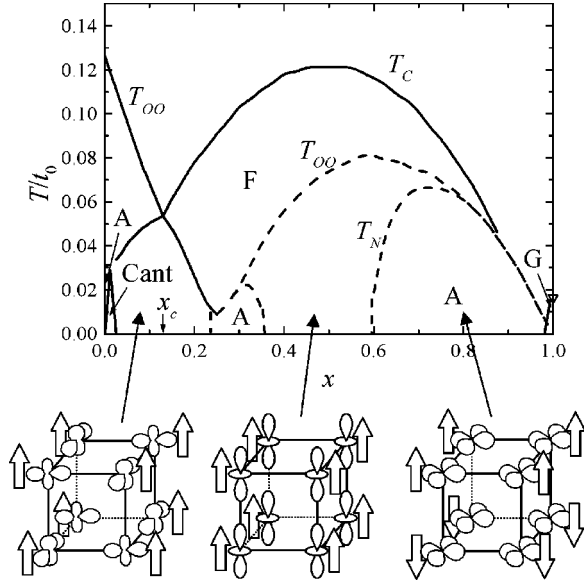


FIG. 1. The spin and orbital phase diagram as a function of hole concentration (x) and temperature (T). The schematic orbital states are also shown. T_C , T_N , and T_{OO} indicate the ferromagnetic Curie temperature, the Néel temperature, and the orbital ordering temperature, respectively. F , A , and G indicate the ferromagnetic, A -type antiferromagnetic, and G -type antiferromagnetic phases, respectively. The solid (broken) lines are for the second- (first-) order phase transitions. The parameter values are chosen to be $J_1/t_0 = 0.25$, $J_2/t_0 = 0.075$, and $J_{AF}/t_0 = 0.0035$.

of the bands. The Fermi energy ε_F is determined by the condition $x = (1/N) \sum_k \sum_l f_F(\varepsilon_k^l - \varepsilon_F)$ where $f_F(\varepsilon)$ is the Fermi distribution function. The mean-field solutions are obtained by minimizing \mathcal{F} with respect to $\tilde{\lambda}_i^u$.

III. NUMERICAL RESULTS

A. Spin and orbital phase diagram at finite temperature

The spin and orbital states at finite T and x are numerically calculated by utilizing the mean-field theory introduced in Sec. II. The four types of spin structure, that is, the ferromagnetic (F), the layer (A)-type AF, the rod (C)-type AF, and the NaCl (G)-type AF structures are considered. As for the orbital, the ferromagneticlike structure, where one kind of orbital exists, and the G -type structure, where two kinds of orbital are alternately aligned in the $[111]$ direction, are considered. The homogeneous phase where the charge carriers are uniformly distributed is assumed unlike the phase-separated state. This is because we have confirmed that stability of phase separation is sensitive to the interactions in the model and the order parameters in the mean-field approximation, although the considered interactions and order parameters in the present calculation are sufficient to investigate roles of the orbital of our interest.

The numerical results are shown in Fig. 1. Parameter values are chosen to be $J_1/t_0 = 0.25$, $J_2/t_0 = 0.075$, and $J_{AF}/t_0 = 0.0035$ which are determined by the analyses of the photoemission experiments²⁹ and the Néel temperature in CaMnO_3 .³⁰ The schematic pictures of the orbital ordered states are also presented. With increasing x from $x=0$, the

spin structure changes as A -type AF $\rightarrow F \rightarrow A$ -type AF $\rightarrow G$ -type AF which is associated with change of the orbital states; in the region of $x \leq 0.25$, the interaction caused by the first term of \mathcal{H}_J is the dominant one between nearest-neighbor orbitals and the G -type AF orbital ordered state is brought about. The type of the orbital favored in this term is denoted as $(\Theta_A^i/\Theta_B^i) = (\pi/2 / -\pi/2)$, where $\Theta_{A(B)}^i$ is the angle of the pseudospin in sublattice $A(B)$ and its definition is the same with θ_i^u in Eq. (7). These orbitals are mixtures of $d_{3x^2-r^2}$ and $d_{y^2-z^2}$, and $d_{3y^2-r^2}$ and $d_{z^2-x^2}$, respectively. Above $x=0.25$, the F -type orbital ordered state is realized. In particular, the $d_{x^2-y^2}$ orbital is uniformly aligned in the A -type AF spin phase above $x=0.6$. A large hopping integral for electrons in the xy plane in this orbital ordered state is energetically favored in the A -type AF state where the hopping in the z direction is prohibited.³¹ The calculated results of the spin and orbital phase diagram at $T=0$ are consistent with those obtained by the Hartree-Fock theory.³¹ The spin and orbital phase diagram at finite T was calculated in Ref. 32 where the Monte Carlo method in a finite-size cluster was used in the spin-orbital-lattice coupled model.

Now, let us focus on the spin ordering temperatures, i.e., T_C and T_N , and the orbital ordering temperature, T_{OO} , in Fig. 1. These ordering temperatures vs x curves qualitatively reproduce the experimental results observed in $\text{La}_{1-x}\text{Sr}_x\text{MnO}_3$ (Refs. 33 and 16), $\text{Pr}_{1-x}\text{Sr}_x\text{MnO}_3$ (Refs. 33 and 15), and $\text{Nd}_{1-x}\text{Sr}_x\text{MnO}_3$ (Ref. 14) except for the narrow region of the charge ordered phase in $\text{Nd}_{0.5}\text{Sr}_{0.5}\text{MnO}_3$. It is shown in Fig. 1 that T_{OO} is higher (lower) than T_C in the region of $x < 0.1$ ($x > 0.1$). The dominant interaction in the region of $x < 0.1$ is provided by \mathcal{H}_J where the effective interaction between spins in the orbital disordered state are given by $3J_1/2$ and $J_1/2$, respectively. Here, the first term in \mathcal{H}_J is considered. Thus, T_{OO} is higher than T_C . On the other hand, in the region where \mathcal{H}_I is dominant, gain of the kinetic energy associated with the long-range ordering causes the transition; it is assumed that doped holes are introduced at the bottom of the band and the kinetic energy is proportional to the bandwidth. The ratio of the bandwidth in the ferromagnetic state to that in the paramagnetic state is obtained as $3/2$ where the orbital disordered state is assumed. On the other hand, the ratio of the bandwidth in the F -type orbital ordered state to that in the orbital disordered state is obtained as $\pi^2/8$, where the spin paramagnetic state is assumed. The energy gain associated with the orbital ordering is smaller than that with the spin one, so that T_C is higher than T_{OO} . This is attributed to the hopping integral between different kinds of orbitals.

Between T_N for the A -type AF state and T_{OO} , the relation $T_N \leq T_{OO}$ is satisfied in the whole region of x in Fig. 1. In addition, the orbital order-disorder transition and the A -type AF one are of the first order in the region of $x > 0.25$. This is numerically confirmed by discontinuity in the orbital (spin) order parameter at T_{OO} (T_N). Both the two results originate from the anisotropy in the pseudospin space as discussed later in more detail.

B. Spin and orbital phase transitions in the lightly doped region

In the lightly doped region in Fig. 1, T_C (T_{OO}) increases (decreases) with increasing x from $x=0$ and the two transi-

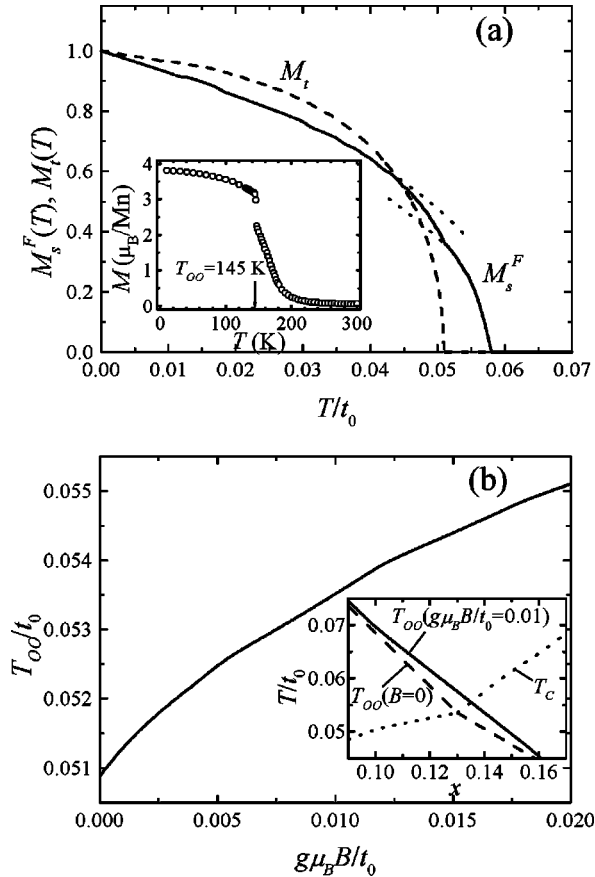


FIG. 2. (a) Temperature dependence of the magnetization M_s^F (solid line) and the orbital order parameter M_t (broken line) at $x=0.14$. The dotted lines are guides to the eyes. The inset shows the magnetization curve in $\text{La}_{0.88}\text{Sr}_{0.12}\text{MnO}_3$ (Ref. 34). (b) Magnetic-field dependence of the orbital ordering temperature T_{OO} at $x=0.14$. The inset shows T_{OO} at $g\mu_B B/t_0=0$ and 0.01 and the ferromagnetic Curie temperature T_C around x_c . Parameter values in the calculation are the same as those in Fig. 1.

tion temperatures cross with each other around $x=0.13$ termed x_c . Around x_c , the coupling between spin and orbital degrees of freedom brings about the unique phase transition as follows. Let us focus on the region where x is slightly higher than x_c . With decreasing T , the system changes from the paramagnetic phase with the orbital disordered state to the ferromagnetic phase and then to the ferromagnetic phase with the orbital ordered state. The temperature dependence of the magnetization at $x=0.14$ is presented in Fig. 2(a) where the order parameter of the orbital ordered state is also plotted. It is shown that the magnetization is enhanced below T_{OO} . This originates from the coupling between the spin and orbital in \mathcal{H}_J [Eq. (3)]; in the mean-field theory, the effective interaction between nearest-neighboring spins is given by $-2J_1(\langle n_i n_j \rangle / 4 - \langle \tau_i^l \tau_j^l \rangle)$ where the first term in \mathcal{H}_J is considered. With taking into account the fact that the orbital ordered state is $(\Theta_A / \Theta_B) = (\pi/2 - \pi/2)$ in this region of x , the effective interaction is rewritten as $-2J_1(1-x)^2(1/4 + 3M_t^2/16)$ for $l=x$ and y and $-2J_1(1-x)^2/4$ for $l=z$. Thus, the magnetization increases below T_{OO} as a result of enhancement of the effective magnetic interaction. In the opposite way, the orbital order-disorder transition is influenced by a change of the spin state. The magnetic-field dependence

of T_{OO} at $x=0.14$ is presented in Fig. 2(b). The inset shows a change of the phase diagram by applying the magnetic field around x_c . T_{OO} increases by applying a magnetic field. The effective interaction between nearest-neighboring orbitals is given by $2J_1(1-x)^2(3/4 + M_t^2/4)$ which increases by applying the magnetic field. This implies that the orbital state is controlled by the magnetic field, although the field is not a canonical external field for the pseudospin.

This unique phase transition originating from the coupling between spin and orbital is observed in manganites.^{19,34} In $\text{La}_{0.88}\text{Sr}_{0.12}\text{MnO}_3$, the ferromagnetic ordering occurs at 175 K and the orbital ordering is confirmed below 145 K by the resonant x-ray scattering which is a direct probe to detect the orbital ordering. The ferromagnetic phase with the orbital disordered state changes into the phase with the orbital ordered state at 145 K, so that it corresponds to the calculated phase transition at T_{OO} around $x=0.14$. It is experimentally confirmed that the magnetization is enhanced below 145 K [the inset of Fig. 2(a)] and the orbital ordering temperature increases with applying the magnetic field.^{35–37,34} These experimental results are well explained by the present calculation and are strong evidences of the novel coupling between spin and orbital in this compound.

C. Phase transition in the highly doped region and the A-type AF metal

In this section, we focus on the phase transition in the highly doped region ($x>0.5$) in Fig. 1 where the A-type AF state associated with the $d_{x^2-y^2}$ orbital ordered state appears. There are two kinds of carrier concentration regions termed region I ($0.8>x>0.6$), where a sequential phase transition from the paramagnetic state to the ferromagnetic state and to the A-type AF state occurs with decreasing T , and region II ($x>0.8$), where the transition from the paramagnetic state to the A-type AF state occurs. The temperature dependences of the spin order parameters at $x=0.725$ (region I) and $x=0.9$ (region II) are shown in Figs. 3(a) and 3(b), respectively. M_s^F and M_s^{AF} are the order parameters of the ferromagnetic and A-type AF spin structures, respectively. As shown in Fig. 3(a), M_s^F appears at $T_C/t_0=0.95$ where the transition is of the second order. With decreasing T , the F -type orbital ordered state with the $d_{x^2-y^2}$ orbital appears at $T_{OO}/t_0=0.72$ and the transition from the ferromagnetic phase to the A-type AF phase occurs at T_N . This transition is of the first order and the canted AF phase does not appear between the ferromagnetic and A-type AF phases. This sequential phase transition is caused by the thermal fluctuation of the orbital; as previously mentioned, the A-type AF state and the F -type orbital ordered state with the $d_{x^2-y^2}$ orbital are cooperatively stabilized at $T=0$. With increasing T , the thermal fluctuation of orbital grows up and the hopping integral in the z direction becomes finite. As a result, the double exchange interaction in this direction overcomes the antiferromagnetic SE interaction and the ferromagnetic phase is stabilized. In region II, the A-type AF ordering and the F -type orbital ordering with the $d_{x^2-y^2}$ orbital occur at the same temperature where the transition is of the first-order as shown in Fig. 3(b). In both the regions I and II, the relation $T_N \leq T_{OO}$ is satisfied. The first order transition at T_{OO} and this relation between T_{OO} and T_N originate from the breaking of the inversion symme-

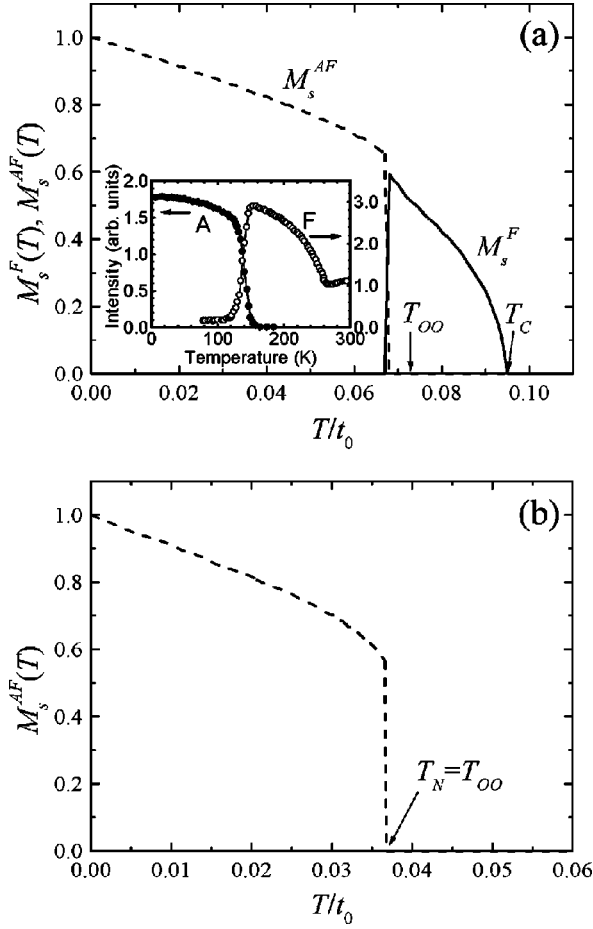


FIG. 3. Temperature dependences of the spin order parameters (a) at $x=0.725$ and (b) at $x=0.9$. The solid and broken lines show the order parameters in the ferromagnetic state (M_s^F) and the A-type antiferromagnetic state (M_s^{AF}), respectively. Parameter values are the same as those in Fig. 1. The inset in (a) shows the temperature dependences of magnetic Bragg reflections in $\text{Pr}_{0.5}\text{Sr}_{0.5}\text{MnO}_3$ (Ref. 13).

try of the system with respect to the orbital pseudospin operator, as discussed in Sec. IV. The calculated results of the sequential phase transition in region I reproduce well the experimental results observed in $\text{Pr}_{0.5}\text{Sr}_{0.5}\text{MnO}_3$ (Ref. 13) [the inset of Fig. 3(a)]. The first-order transition at T_{OO} ($=T_N$) in region II is consistent with the experiments in $\text{Nd}_{0.45}\text{Sr}_{0.55}\text{MnO}_3$ (Refs. 13 and 14), where the Mn-O bond length in the z direction (xy plane) is confirmed to become short (long) at T_N .³⁸ It implies the F -type orbital ordering with the $d_{x^2-y^2}$ orbital as predicted from the present calculation.

In the actual compounds, where the A-type AF state is observed, the tetragonal lattice distortion is observed and the cubic symmetry is broken far above T_N .^{13,38} We simulate this distortion by introducing the uniaxial anisotropy of the hopping integral and the SE interaction and investigate the phase transition. It is assumed that $t_0^{xy}/t_0^z = \sqrt{J_{AF}^{xy}/J_{AF}^z} = R$, where $t_0^{xy(z)}$ and $J_{AF}^{xy(z)}$ are the hopping integral and the antiferromagnetic SE interaction in the xy plane (z direction). The temperature dependences of the spin and orbital order parameters at $x=0.725$ and 0.9 with $R=1.2$ are shown in Figs. 4(a) and 4(b), respectively. Due to the uniaxial anisotropy,

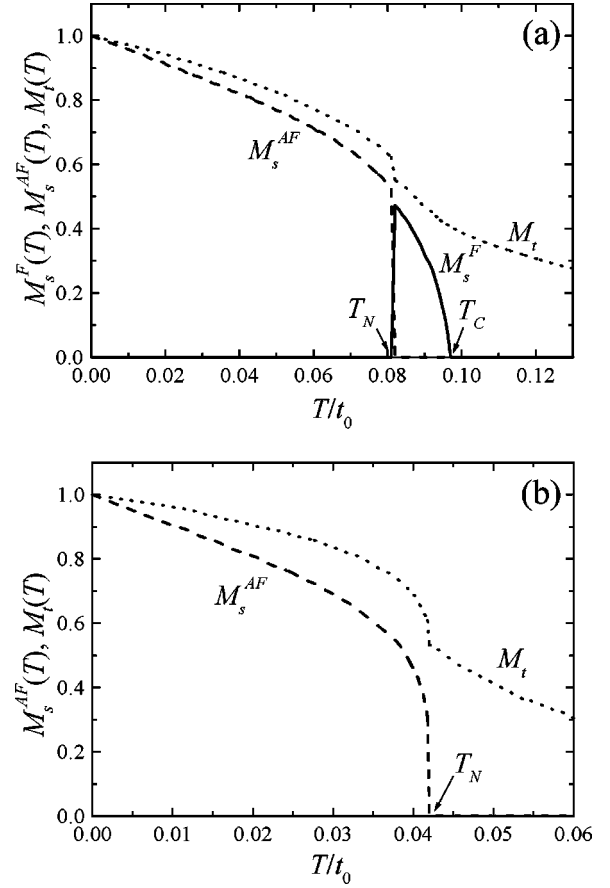


FIG. 4. Temperature dependences of the spin and orbital order parameters (a) at $x=0.725$ and (b) at $x=0.9$ in the tetragonal lattice. The solid, broken, and dotted lines show the order parameters for the ferromagnetic structure (M_s^F), the A-type AF structure (M_s^{AF}), and the F -type orbital ordered structure (M_t), respectively. The uniaxial anisotropy is introduced as $t_0^{xy}/t_0^z = \sqrt{J_{AF}^{xy}/J_{AF}^z} = R$ with $R=1.2$, where $t_0^{xy(z)}$ and $J_{AF}^{xy(z)}$ are the hopping integral and the antiferromagnetic SE interaction in the xy plane (the z direction). The other parameter values are the same as those in Fig. 1.

M_t is finite above the orbital ordering temperature in the system with the cubic symmetry. It is worth noting that (1) T_N for the A-type AF state increases and (2) the transition at T_N is of the first order, although the discontinuity of M_s^{AF} is reduced. The latter is attributed to diminution of the change of M_t at T_N .

Finally, the magnetic-field dependence of T_{OO} is shown in Fig. 5. T_{OO} decreases with applying the magnetic field in the region of $g\mu_B B/t_0 < 0.0025$ where the nearest-neighboring spins in the z direction are canted. The spins become parallel at $g\mu_B B/t_0 = 0.0025$ termed B_c , and T_{OO} increases with increasing the magnetic field above B_c . The orbital ordered state below T_{OO} is of the F type with the $d_{x^2-y^2}$ orbital and does not depend on the magnitude of the magnetic field. Above and below B_c , the different mechanisms dominate the magnetic field dependence of T_{OO} ; in the region of $B < B_c$, the spin canting due to the magnetic-field promotes the electron hopping in the z axis which weakens the orbital ordered state. On the other hand, above B_c , magnitude of the magnetic moment is enhanced by increasing the magnetic field and the orbital ordered state associated with the ferromagnetic spin structure is stabilized.

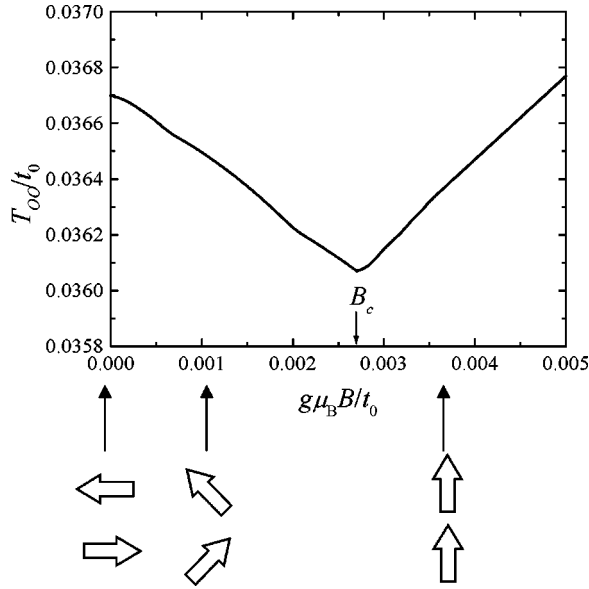


FIG. 5. Magnetic-field dependence of the orbital ordering temperature at $x=0.9$ and the schematic spin configurations. Parameter values are the same as those in Fig. 1.

The magnetic-field dependence of T_N for the A -type AF spin structure is recently measured in $\text{Nd}_{0.45}\text{Sr}_{0.55}\text{MnO}_3$.¹⁴ It is experimentally shown that T_N gradually decreases with increasing the magnetic field. From the present calculation, it is predicted that this reduction of T_N is accompanied with that of T_{OO} , and with increasing the magnetic field furthermore, T_{OO} increases above the critical value of the field.

IV. FIRST-ORDER PHASE TRANSITION AND ORBITAL DEGREE OF FREEDOM

As mentioned in Sec. III, several characteristics of the phase transitions in manganites are attributed to the unique properties of the orbital degree of freedom. In this section we study analytically the phase transition by expanding the free energy with respect to the spin and orbital order parameters.²⁵ Let us consider the ferromagnetic and A -type AF spin structures and the F -type and G -type AF orbital structures. The expectation values of the Hamiltonian at finite temperature are calculated by the mean-field theory introduced in Sec. II and are expanded with respect to M_s and M_t . It is assumed that doped holes are introduced at the bottom of the band denoted by ε_k^l in Eq. (14). The explicit form of $\langle \mathcal{H}_J \rangle_{st}$ is given by

$$\frac{\langle \mathcal{H}_J \rangle_{st}}{N} = -\frac{(1-x)^2}{2} \sum_{l=x,y,z} \{J_1(3 + \cos \Theta_l^s M_s^2)(1 - A_{2l} M_t^2) + J_2(1 - \cos \Theta_l^s M_s^2)(3 + A_{1l} M_t + A_{2l} M_t^2)\}, \quad (15)$$

where

$$A_{1l} = 2(C_{Al} + C_{Bl}) \quad (16)$$

and

$$A_{2l} = C_{Al} C_{Bl}, \quad (17)$$

with $C_{A(B)l} = \cos(\Theta_{A(B)l}^t + 2\pi m_l/3)$ and $(m_x, m_y, m_z) = (1, -1, 0)$. Θ_l^s ($l=x, y, z$) is the relative angle between nearest-neighboring spins in direction l and $\Theta_{A(B)l}^t$ is the angle of the orbital pseudospin in sublattice $A(B)$. $\langle \mathcal{H}_t \rangle_{st}$ is proportional to the bandwidth W of the spinless and orbital-less fermion as

$$\frac{\langle \mathcal{H}_t \rangle_{st}}{N} = -x \frac{W}{2}, \quad (18)$$

and is expanded with respect to M_s and M_t up to the orders of M_s^2 and M_t^3 as follows:

$$\frac{\langle \mathcal{H}_t \rangle_{st}}{N} = -t_0 x \frac{16}{3\pi^2} \sum_{l=x,y,z} \left(1 + \frac{3}{5} \cos \Theta_l^s M_s^2 \right) (1 + \alpha_{1l} M_t + \alpha_{2l} M_t^2 + \alpha_{3l} M_t^3), \quad (19)$$

where

$$\alpha_{1l} = \frac{2}{3}(C_{Al} + C_{Bl}), \quad (20)$$

$$\alpha_{2l} = \frac{2}{15}(1 - C_{Al}^2 - C_{Bl}^2) + \frac{4}{9} C_{Al} C_{Bl}, \quad (21)$$

and

$$\alpha_{3l} = \frac{4}{105}(C_{Al}^3 + C_{Bl}^3) - \frac{4}{45}(C_{Al}^2 C_{Bl} + C_{Al} C_{Bl}^2) + \frac{1}{63}(C_{Al} + C_{Bl}). \quad (22)$$

The detailed derivation of Eq. (19) is presented in the Appendix. It is worth noting that the terms which are proportional to M_t or M_t^3 appear in $\langle \mathcal{H}_J \rangle_{st}$ and $\langle \mathcal{H}_t \rangle_{st}$. This is because the inversion symmetry in the system with respect to the orbital pseudospin is broken, i.e., the free energy with $T_z = 1/2$ is different from that with $T_z = -1/2$. This is highly in contrast to the spin case where the inversion symmetry with respect to the spin operator is preserved due to the time-reversal symmetry in the system without a magnetic field. Being based on Eqs. (15) and (19), we investigate the phase transition in the F and A -type AF spin structures in more detail.

Ferromagnetic structure. Equations (15) and (19) with the relation $\Theta_l^s = 0$ for $l=x, y, z$ are given by

$$\frac{\langle \mathcal{H}_J \rangle_{st}}{N} = -(1-x)^2 \frac{3}{8} J_1 (3 + M_s^2) (1 + B_2 M_t^2) - (1-x)^2 \frac{3}{8} J_2 (1 - M_s^2) (3 - B_2 M_t^2) \quad (23)$$

and

$$\frac{\langle \mathcal{H}_t \rangle_{st}}{N} = -t_0 x \frac{16}{\pi^2} \left(1 + \frac{3}{5} M_s^2 \right) (1 + \beta_2 M_t^2 + \beta_3 M_t^3), \quad (24)$$

respectively, with

$$B_2 = -\frac{1}{2} \cos(\Theta_A^t - \Theta_B^t), \quad (25)$$

$$\beta_2 = \frac{2}{9} \cos(\Theta_A^t - \Theta_B^t), \quad (26)$$

and

$$\begin{aligned} \beta_3 = & \frac{4}{105} (\cos^3 \Theta_A^t + \cos^3 \Theta_B^t) - \frac{1}{35} (\cos \Theta_A^t + \cos \Theta_B^t) \\ & - \frac{1}{45} [\cos(2\Theta_A^t + \Theta_B^t) + \cos(\Theta_A^t + 2\Theta_B^t)]. \quad (27) \end{aligned}$$

The terms being proportional to M_t vanish due to the cubic symmetry of the ferromagnetic spin structure. The coefficients B_2 and β_2 become the largest at $\Theta_A^t = \Theta_B^t - \pi$ and at $\Theta_A^t = \Theta_B^t$, respectively. That is, \mathcal{H}_J and \mathcal{H}_t favor AF- and F-type orbital ordered states, respectively.

Let us focus on the term being proportional to M_t^3 in $\langle \mathcal{H}_t \rangle_{st}$. In the case where this term is relevant, the orbital order-disorder transition is of the first-order according to the Landau criterion in the phase transition. It corresponds to the transition at T_{OO} in the region of $x > 0.25$ in Fig. 1 and is consistent with the first-order transitions at the orbital ordering temperature observed in several manganites. On the other hand, the transition in the region of $x < 0.25$ in Fig. 1 is of the second order. This is because (1) the term being proportional to M_t^3 does not appear in $\langle \mathcal{H}_J \rangle_{st}$, and (2) in this hole concentration region, the G-type orbital ordered state with $\Theta_A^t = \Theta_B^t - \pi$ is realized. The inversion symmetry with respect to the pseudospin operator is preserved, i.e., $\beta_3 = 0$ in Eq. (27) in this orbital ordered state. The phase transition in this hole concentration region is discussed in more detail in Sec. V. The first-order transition in the cooperative JT system and its relation to the terms proportional to Q^3 , where Q indicates the normal mode of a MnO_6 octahedron, was discussed in Ref. 39.

The parameter β_3 becomes the largest at $\Theta_A^t = \Theta_B^t = (2n + 1)\pi/3$ with $n = (1, 2, 3)$ and determines the orbital state uniquely. With taking into account β_2 together with β_3 , $\langle \mathcal{H}_t \rangle_{st}$ favors the F-type orbital ordered state with $d_{x^2-y^2}$, $d_{y^2-z^2}$, and $d_{z^2-x^2}$ (the so-called leaf-type orbital) rather than $d_{3x^2-r^2}$, $d_{3x^2-r^2}$, and $d_{3y^2-r^2}$ (the so-called cigar-type orbital). Since the bandwidth in the F-type orbital ordered state at $T=0$ does not depend on types of the orbital, the thermal fluctuation stabilizes the leaf-type orbital; the F-type orbital ordered state with $d_{x^2-y^2}$ ($d_{3z^2-r^2}$) mixes with the AF-type one with ($d_{3x^2-r^2}/d_{3y^2-r^2}$) [$(d_{y^2-z^2}/d_{z^2-x^2})$] through the thermal fluctuation. The bandwidth in the ($d_{3x^2-r^2}/d_{3y^2-r^2}$) state is $5t_0$ which is larger than that in the ($d_{y^2-z^2}/d_{z^2-x^2}$) state ($3t_0$). The smaller bandwidth in the latter state is attributed to the fact that the hopping integral in the xy plane is zero in this orbital state.

A-type AF structure. In this spin structure, $\langle \mathcal{H}_J \rangle_{st}$ and $\langle \mathcal{H}_t \rangle_{st}$ with $\Theta_x^s = \Theta_y^s = 0$ and $\Theta_z^s = \pi$ are given by

$$\frac{\langle \mathcal{H}_J \rangle_{st}}{N} = (1-x)^2 \frac{1}{16} (J_1 D_1 + J_2 D_2) \quad (28)$$

with

$$\begin{aligned} D_1 = & -18 - 2M_s^2 + 9 \cos(\Theta_A^t - \Theta_B^t) M_t^2 \\ & + [3 \cos(\Theta_A^t - \Theta_B^t) - 2 \cos \Theta_A^t \cos \Theta_B^t] M_s^2 M_t^2, \quad (29) \end{aligned}$$

and

$$\begin{aligned} D_2 = & -18 + 6M_s^2 - 3 \cos(\Theta_A^t - \Theta_B^t) M_t^2 \\ & - 4(\cos \Theta_A^t + \cos \Theta_B^t) M_s^2 M_t \\ & + [3 \cos(\Theta_A^t - \Theta_B^t) - 2 \cos \Theta_A^t \cos \Theta_B^t] M_s^2 M_t^2 \quad (30) \end{aligned}$$

and

$$\frac{\langle \mathcal{H}_t \rangle_{st}}{N} = -t_0 x \left(\frac{16}{\pi^2} \right) \left(1 + \frac{1}{5} M_s^2 + \gamma_1 M_s^2 M_t + \beta_2 M_t^2 + \beta_3 M_t^3 \right) \quad (31)$$

with

$$\gamma_1 = -\frac{4}{15} (\cos \Theta_A^t + \cos \Theta_B^t), \quad (32)$$

respectively. The most remarkable difference of the results in the A-type AF structure from that in the ferromagnetic one is the terms being proportional to $M_s^2 M_t$. The origin of these terms is the anisotropic spin structure in the A-type AF state which breaks the cubic symmetry in the system. Because of these terms, the order parameter of the A-type AF state acts as a magnetic field on the orbital pseudospin space and the relation $T_{OO} \geq T_N$ is derived. This relation is seen in the present phase diagram (Fig. 1) and also in the experimental results in several manganites.

Now we focus on these terms being proportional to $M_t M_s^2$. At $x=0$ where \mathcal{H}_J is dominant, the AF-type orbital ordered states with $(\Theta^t/\Theta^t + \pi)$ for any Θ^t is realized above T_N . Below T_N , the term being proportional to $M_s^2 M_t$ becomes relevant and the orbital state is uniquely determined as $(\Theta^t/-\Theta^t)$ with

$$\Theta^t = \cos^{-1} \frac{4J_2 M_s^2}{3(3J_1 - J_2)M_t + (J_1 + J_2)M_s^2 M_t}. \quad (33)$$

With decreasing temperature below T_N , Θ^t continuously changes from $\pi/2$ at T_N to $\cos^{-1}\{2J_2/(5J_1 - J_2)\}$ at $T=0$. This orbital state favors the antiferromagnetic interaction in the z direction in this spin structure. In the present calculation, the ferromagnetic interaction in the xy plane originates from J_1 and the AF structure in the z direction from J_2 and J_{AF} .^{17,31,21} It was reported by the model without the antiferromagnetic SE interaction J_{AF} that this spin structure competes with the planar ferromagnetic structure and its stability depends on types of the occupied orbitals.⁴⁰ Due to J_{AF} in the present model, the A-type AF structure is more stabilized than the planar ferromagnetic one in the wide range of Θ^t . In the highly doped region where \mathcal{H}_t is dominant, the term $\gamma_1 M_s^2 M_t$ in Eq. (31) favors the F-type orbital ordered state with $\Theta_A^t = \Theta_B^t = \pi$ which corresponds to the state with $d_{x^2-y^2}$, as mentioned in Sec. IV A. The terms being proportional to $M_s^2 M_t$ also appear in the C-type AF spin structure

where the relation $T_{OO} \geq T_N$ is derived. The coefficients of the term in $\langle \mathcal{H}_J \rangle_{st}$ and $\langle \mathcal{H}_t \rangle_{st}$ are given by $J_2(1-x)^2(\cos \Theta_A^t + \cos \Theta_B^t)/2$ and $-t_0 x 32(\cos \Theta_A^t + \cos \Theta_B^t)/(5\pi^2)$ which favor the G type with $(d_{3z^2-r^2}/d_{x^2-y^2})$ and the F type with $d_{3z^2-r^2}$ orbital ordered states, respectively.

V. SUMMARY AND DISCUSSION

In this paper we study roles of the orbital degree of freedom in phase transition in perovskite manganites. The effective Hamiltonian, which includes the orbital degree of freedom as well as the spin and charge degrees of freedom, is utilized and the mean-field theory at finite temperature and carrier concentration is adopted. Through both the numerical and analytical calculations based on this theory, it is revealed that several characteristics of the phase transition observed in manganites originate from the unique properties of the orbital degree of freedom. The obtained results are summarized as follows: (1) The orbital order-disorder transition is of the first order in the wide region of x , and T_N for the anisotropic spin structure, such as the A - and C -type AF structures, is lower than T_{OO} . Both the results originate from the fact that the inversion symmetry in the system is broken with respect to the orbital pseudospin operator and the terms being proportional to $M_s^2 M_t$ and M_t^3 exist in the free energy. These results are consistent with the phase transition observed in $\text{Pr}_{0.5}\text{Sr}_{0.5}\text{MnO}_3$ and $\text{Nd}_{0.45}\text{Sr}_{0.55}\text{MnO}_3$ (Refs. 13, 14, and 38) where the A -type AF state with the $d_{x^2-y^2}$ orbital ordered state appears. In the present calculation, the phase transition at T_{OO} in the region of $x < 0.25$ is of the second order as shown in Fig. 1. With taking into account the following ingredients, the phase transition changes from the second-order transition to the first-order transition: (a) the higher-order coupling between the pseudospin and the JT-type distortion in a MnO_6 octahedron, (b) the anharmonic term of the potential energy for the JT-type lattice distortion,³⁹ and (c) the higher-order terms with respect to t_0/U in the effective Hamiltonian in Eq. (1). It was shown by the neutron diffraction¹¹ and the resonant x-ray scattering experiments¹² that the orbital order-disorder transition in LaMnO_3 at 780 K is of the first order but is close to the second order. Therefore, these contributions are supposed to be small or almost canceled out with each other. (2) The relation $T_C > T_{OO}$ is satisfied in the highly hole doped region ($x > 0.1$). This is because gain of the kinetic energy of electrons accompanied with the orbital ordering is lower than that with the ferromagnetic ordering due to the hopping integral between different kinds of orbitals, unlike the spin case. (3) In the region where T_{OO} and T_C are close with each other, the novel phase transition is brought about due to the coupling between the spin and orbital degrees of freedom. The magnetization is enhanced below T_{OO} and T_{OO} increases by applying the magnetic field. These results well explain the unique experimental results observed in $\text{La}_{0.88}\text{Sr}_{0.12}\text{MnO}_3$. (4) The sequential phase transition from the A -type AF phase to the ferromagnetic phase with increasing T is caused by the thermal fluctuation of the orbital from the $d_{x^2-y^2}$ orbital ordered states. The ferromagnetic interaction in the z axis becomes finite due to the orbital fluctuation.

ACKNOWLEDGMENTS

The authors would like to thank Y. Endoh, K. Hirota, H. Nojiri, Y. Murakami, and Y. Tokura for their valuable discussions. This work was supported by CREST (Core Research for Evolutional Science and Technology Corporation) Japan, NEDO (New Energy Industrial Technology Development Organization) Japan, and Grant-in-Aid for Scientific Research Priority Area from the Ministry of Education, Science and Culture of Japan. S.O. acknowledges the financial support of JSPS. Part of the numerical calculation was performed in the HITACS-3800/380 supercomputing facilities in IMR, Tohoku University.

APPENDIX: EXPANSION OF $\langle \mathcal{H}_t \rangle_{st}$

In this appendix, we present the derivation of Eq. (19), i.e., the expansion of $\langle \mathcal{H}_t \rangle_{st}$ with respect to the spin and orbital order parameters. We start from Eq. (18) where the bandwidth W is calculated from Eq. (13) as follows:

$$W = 2 \sum_{\delta} I_{\delta}^s I'_{\delta}, \quad (\text{A1})$$

where

$$I_{\delta}^s = \sum_{\sigma} \langle |z_{i\sigma}^{s*} z_{j\sigma}^s| \rangle_s \quad (\text{A2})$$

and

$$I'_{\delta} = \sum_{\sigma} \langle |z_{i\gamma}^{t*} t_{ij}^{\gamma\gamma'} z_{j\gamma'}^t| \rangle_t. \quad (\text{A3})$$

Here δ indicates a vector connecting site i and its nearest-neighbor site j . The spin part I_{δ}^s has the same form with Eq. (27) in Ref. 25 and is given by

$$I_{\delta}^s = \frac{2}{3} \left(1 + \frac{3}{5} \cos \Theta_{\delta}^s M_s^2 \right), \quad (\text{A4})$$

where Θ_{δ}^s is the relative angle between spins at sites i and j and the relation $M_s = \lambda^s/3 + O(\lambda^{s3})$ is used. As for the orbital part, we present the derivation of I'_{δ} with $\delta = \pm a\hat{z}$ termed I'_z , where a and \hat{z} indicate a cell parameter of the cubic perovskite lattice and the unit vector in the z direction, respectively. I'_{δ} with $\delta = \pm a\hat{x}(\hat{y})$ is given by I'_z , where Θ_i^t is replaced by $\Theta_i^t + 2\pi/3$ ($\Theta_i^t - 2\pi/3$). I'_z is calculated as

$$\begin{aligned} I'_z &= t_0 \left\langle \left| \cos \frac{\theta_i^t}{2} \cos \frac{\theta_j^t}{2} \right| \right\rangle_t \\ &= \frac{t_0}{v^{t2}} \int_0^{2\pi} d\delta\theta_i \int_0^{2\pi} d\delta\theta_j e^{\lambda^t(\cos \delta\theta_i + \cos \delta\theta_j)} \\ &\quad \times \left| \cos \frac{\Theta_i^t + \delta\theta_i}{2} \cos \frac{\Theta_j^t + \delta\theta_j}{2} \right|, \end{aligned} \quad (\text{A5})$$

where $\delta\theta_i = \theta_i^t - \Theta_i^t$. The right-hand side of Eq. (A5) is expanded with respect to λ^t up to the order of $O(\lambda^{t3})$ as follows:

$$I_z^t = \frac{t_0}{(2\pi)^2} \left(1 - \frac{\lambda^{t2}}{4}\right)^2 \left(\zeta_{i0} + \zeta_{i1}\lambda^t + \frac{\zeta_{i2}}{2!}\lambda^{t2} + \frac{\zeta_{i3}}{3!}\lambda^{t3} \right) \times \left(\zeta_{j0} + \zeta_{j1}\lambda^t + \frac{\zeta_{j2}}{2!}\lambda^{t2} + \frac{\zeta_{j3}}{3!}\lambda^{t3} \right), \quad (\text{A6})$$

where ζ_{in} ($n=0\sim 3$) are given by

$$\zeta_{i0} = 4, \quad (\text{A7})$$

$$\zeta_{i1} = \frac{4}{3} \cos \Theta_i^t, \quad (\text{A8})$$

$$\zeta_{i2} = \frac{4}{15} (8 - \cos^2 \Theta_i^t), \quad (\text{A9})$$

and

$$\zeta_{i3} = \frac{4}{35} (\cos^3 \Theta_i^t + 8 \cos \Theta_i^t). \quad (\text{A10})$$

The relation $\nu^t = 2\pi(1 + \frac{1}{4}\lambda^{t2}) + O(\lambda^{t4})$ is used. In the G-type orbital ordered state considered in Sec. III, Θ_i^t in the above formulas is replaced by $\Theta_{A(B)}^t$, when site i belongs to the orbital sublattice $A(B)$. By utilizing the relation $M_t = \lambda^t/2 - \lambda^{t3}/16 + O(\lambda^{t5})$, Eq. (19) is derived.

- ¹K. Chahara, T. Ohono, M. Kasai, Y. Kanke, and Y. Kozono, *Appl. Phys. Lett.* **62**, 780 (1993).
- ²R. von Helmolt, J. Wecker, B. Holzapfel, L. Schultz, and K. Samwer, *Phys. Rev. Lett.* **71**, 2331 (1993).
- ³Y. Tokura, A. Urushibara, Y. Moritomo, T. Arima, A. Asamitsu, G. Kido, and N. Furukawa, *J. Phys. Soc. Jpn.* **63**, 3931 (1994).
- ⁴S. Jin, T. H. Tiefel, M. McCormack, R. A. Fastnacht, R. Ramesh, and L. H. Chen, *Science* **264**, 413 (1994).
- ⁵Y. Tomioka, A. Asamitsu, Y. Moritomo, and Y. Tokura, *J. Phys. Soc. Jpn.* **64**, 3626 (1995).
- ⁶P. Schiffer, A. P. Ramirez, W. Bao, and S. -W. Cheong, *Phys. Rev. Lett.* **75**, 3336 (1995).
- ⁷A. J. Millis, P. B. Littlewood, and B. I. Shraiman, *Phys. Rev. Lett.* **74**, 5144 (1995).
- ⁸J. B. Goodenough, *Phys. Rev.* **100**, 564 (1955); in *Progress in Solid State Chemistry*, edited by H. Reiss (Pergamon, London, 1971), Vol. 5.
- ⁹J. Kanamori, *J. Phys. Chem. Solids* **10**, 87 (1959).
- ¹⁰G. Matsumoto, *J. Phys. Soc. Jpn.* **29**, 606 (1970).
- ¹¹J. Rodriguez-Carvajal, M. Hennion, F. Moussa, and A. H. Moudden, *Phys. Rev. B* **57**, R3189 (1998).
- ¹²Y. Murakami, J. P. Hill, D. Gibbs, M. Blume, I. Koyama, M. Tanaka, H. Kawata, T. Arima, Y. Tokura, K. Hirota, and Y. Endoh, *Phys. Rev. Lett.* **81**, 582 (1998).
- ¹³H. Kawano, R. Kajimoto, H. Yoshizawa, Y. Tomioka, H. Kuwahara, and Y. Tokura, *Phys. Rev. Lett.* **78**, 4253 (1997).
- ¹⁴H. Kuwahara, T. Okuda, Y. Tomioka, A. Asamitsu, and Y. Tokura, *Phys. Rev. Lett.* **82**, 4316 (1999); in *Science and Technology of Magnetic Oxides*, edited by M. Hundley, J. Nickel, R. Ramesh, and Y. Tokura, MRS Symposia Proceedings No. 494 (Materials Research Society, Pittsburgh, 1998), p. 83.
- ¹⁵Y. Tomioka and Y. Tokura (unpublished).
- ¹⁶T. Akimoto, Y. Maruyama, Y. Moritomo, A. Nakamura, K. Hirota, K. Ohoyama, and M. Ohashi, *Phys. Rev. B* **57**, R5594 (1998).
- ¹⁷S. Ishihara, J. Inoue, and S. Maekawa, *Physica C* **263**, 130 (1996); *Phys. Rev. B* **55**, 8280 (1997).
- ¹⁸J. C. Slater and G. F. Koster, *Phys. Rev.* **94**, 1498 (1954); W. A. Harrison, in *Electronic Structure and the Properties of Solids, The Physics of the Chemical Bond* (W.H. Freeman and Company, San Francisco, 1980).
- ¹⁹Y. Endoh, K. Hirota, S. Ishihara, S. Okamoto, Y. Murakami, A. Nishizawa, T. Fukuda, H. Kimura, H. Nojiri, K. Kaneko, and S. Maekawa, *Phys. Rev. Lett.* **82**, 4328 (1999).
- ²⁰L. M. Roth, *Phys. Rev.* **149**, 306 (1966).
- ²¹K. I. Kugel and D. I. Khomskii, *Zh. Eksp. Teor. Fiz. Pis'ma Red.* **15**, 629 (1972) [*JETP Lett.* **15**, 446 (1972)].
- ²²M. Cyrot and C. Lyon-Caen, *J. Phys. (Paris)* **36**, 253 (1975).
- ²³S. Inagaki, *J. Phys. Soc. Jpn.* **39**, 596 (1975).
- ²⁴H. Kawano, R. Kajimoto, M. Kubota, and H. Yoshizawa, *Phys. Rev. B* **53**, R14 709 (1996).
- ²⁵P. G. de Gennes, *Phys. Rev.* **118**, 141 (1960).
- ²⁶S. Okamoto, S. Ishihara, and S. Maekawa, *Phys. Rev. B* **61**, 451 (2000).
- ²⁷S. Ishihara, M. Yamanaka, and N. Nagaosa, *Phys. Rev. B* **56**, 686 (1997).
- ²⁸S. Ishihara, S. Okamoto, and S. Maekawa, *J. Phys. Soc. Jpn.* **66**, 2965 (1997).
- ²⁹T. Saitoh, A. E. Bocquet, T. Mizokawa, H. Namatame, A. Fujimori, M. Abbate, Y. Takeda, and M. Takano, *Phys. Rev. B* **51**, 13 942 (1995).
- ³⁰E. O. Wollan and W. C. Koehler, *Phys. Rev.* **100**, 545 (1955).
- ³¹R. Maezono, S. Ishihara, and N. Nagaosa, *Phys. Rev. B* **57**, R13 993 (1998); **58**, 11 583 (1998).
- ³²L. Sheng and C. S. Ting, *Phys. Rev. B* **60**, 14 809 (1999).
- ³³Y. Tokura, *J. Appl. Phys.* **79**, 5288 (1996).
- ³⁴H. Nojiri, K. Kaneko, M. Motokawa, K. Hirota, Y. Endoh, and K. Takahashi, *Phys. Rev. B* **60**, 4142 (1999).
- ³⁵R. Senis, V. Laukhin, B. Martínez, J. Fontcuberta, X. Obradors, A. A. Arsenov, and Y. M. Mukovskii, *Phys. Rev. B* **57**, 14 680 (1998).
- ³⁶K. Ghosh, R. L. Greene, S. E. Lofland, S. M. Bhagat, S. G. Karabashev, D. A. Shulyatev, A. A. Arsenov, and Y. Mukovskii, *Phys. Rev. B* **58**, 8206 (1998).
- ³⁷S. Uhlenbruck, R. Teipen, R. Klingeler, B. Büchner, O. Friedt, M. Hücker, H. Kierspel, T. Niemöller, L. Pinsard, A. Revolevshii, and R. Gross, *Phys. Rev. Lett.* **82**, 185 (1999).
- ³⁸R. Kajimoto, H. Yoshizawa, H. Kawano, H. Kuwahara, Y. Tokura, K. Ohoyama, and M. Ohashi, *Phys. Rev. B* **60**, 9506 (1999).
- ³⁹M. Kataoka and J. Kanamori, *J. Phys. Soc. Jpn.* **32**, 113 (1972).
- ⁴⁰D. Feinberg, P. Germain, M. Grill, and G. Seibold, *Phys. Rev. B* **57**, R5583 (1998).